Hexagonal images processing over finite Eisenstein fields

Article *in* Procedia Engineering · September 2017

DOI: 10.1016/j.proeng.2017.09.633

2 authors:

Alexander Karkishchenko
Southern Federal University

Valeriy Mnukhin
Southern Federal University

Available online at www.sciencedirect.com

ScienceDirect

Procedia Engineering 201 (2017) 287–295

Procedia Engineering

www.elsevier.com/locate/procedia

3rd International Conference "Information Technology and Nanotechnology (ITNT-2017)", 25-27 April 2017, Samara, Russia

Hexagonal images processing over finite Eisenstein fields

Alexander Karkishchenko[a], Valeriy Mnukhin[a,*]

[a]*Southern Federal University, 105/42, Bolshaya Sadovaya, 344006, Rostov-na-Donu, Russia*

Abstract

This paper considers a new algebraic method for analysis and processing of hexagonally sampled images. The method is based on the interpretation of such images as functions on "Eisenstein fields". These are finite fields $\mathbb{GF}(p^2)$ of special characteristics $p = 12k + 5$, where $k > 0$ is an integer. Some properties of such fields are studied; in particular, it is shown that its elements may be considered as "discrete Eisenstein numbers" and are in natural correspondence with hexagons in a $(p \times p)$-diamond-shaped fragment of a regular plane tiling. We show that in some cases multiplications in Eisenstein fields correspond to rotations combined with appropriate scalings, and use this fact for hexagonal images sharpening, smoothering and segmentation. The proposed algorithms have complexity $O(p^2)$ and can be used also for processing of square-sampled digital images over finite Gaussian fields.

Keywords: hexagonal image; processing; Eisenstein numbers; finite fields; rotations; sharpening; smoothering; segmentation

1. Introduction

Hexagonal sampling (as in Fig. 1) is not new and has been explored by many researchers [1–5]. Indeed, it is known [1] that hexagonal lattice has some advantages over the square lattice which can have implications for analysis of images defined on it. These advantages are as follows:

- **Isoperimetry**. As per the honeycomb conjecture, a hexagon encloses more area than any other closed planar curve of equal perimeter, except a circle.
- **Additional equidistant neighbours**. Every hexagonal pixel has six equidistant neighbours with a shared edge. In contrast, a square pixel has only four equidistant neighbours with a shared edge or a corner. This implies that curves can be represented in a better fashion on the hexagonal lattice.
- **Additional symmetry axes**. Every hexagon in the lattice has 6 symmetry axes in contrast with squares, which have only 4 axes. This implies that there will be less ambiguity in detecting symmetry of images.

* Corresponding author. Tel.: +7-988-569-2926
E-mail address: mnukhin.valeriy@mail.ru

10.1016/j.proeng.2017.09.633

Fig. 1. An example of hexagonal image.

In general, the hexagonal structure provides a more flexible and efficient way to perform image translation and rotation without losing image information [6] and demonstrate the ability to better represent curved structures [7].

A considerable amount of research in hexagonally sampled images processing is taking place now despite the fact that there are no hardware resources that currently produce or display hexagonal images. For this, software resampling is in use, when the original data is sampled on a square lattice while the desired image is to be sampled on a hexagonal lattice; in particular, it has been used to produce examples for the current paper. (Note that for the sake of brevity, the terms *square image* and *hexagonal image* will be used throughout to refer to images sampled on a square lattice and hexagonal lattice, respectively.)

When developing algorithms for image analysis, both in square and hexagonal grid, it is quite common to proceed on the assumption of continuity of images. Then powerful tools of continual mathematics, such as complex analysis and integral transforms, can be efficiently used. However, its application to digital images often leads to systematic errors associated with the inability to adequately transfer some concepts of continuous mathematics to the discrete plane. As an example we can point to the concept of rotation in the plane. Being natural and elementary in the continuous case, it lose these qualities when one tries to define it accurately on a discrete plane. As a result, formal application of continuous methods to digital images could be complicated by systematic errors. This raises the issue of the development of methods initially focused on discrete images and based on tools of algebra and number theory.

One of such methods is considered in this paper. It is based on the interpretation of hexagonal images as functions on "Eisenstein fields". These are finite fields $\mathbb{GF}(p^2)$ of special characteristics $p = 12k+5$, where $0 \le k \in \mathbb{Z}$. We show that elements of such fields may be considered as "discrete Eisenstein numbers" and are in natural correspondence with hexagons in a $(p \times p)$-diamond-shaped fragment of a regular plane tiling. Hence, functions on Eisenstein fields may be considered as hexagonal images of sizes $(p \times p)$, where $p = 5, 17, \ldots, 257, \ldots, 509$, ets. (Note that it is not a limitation since every image can be trivially extended to an appropriate size.)

The significance of such approach is based on the fact that Eisenstein fields inherit some properties of the continuous complex field $\mathbb{C}$. In particular, it is well-known that in the complex plane multiplications may be considered as rotations combined with appropriate scalings. We show that in some respects it is true also for multiplication in Eisenstein fields. Namely, it occurs that though in general such multiplication do produce considerable distortion of images, in some special cases a resulting image consists of several fragments, visually similar to the original one rotated and zoomed out. We use the fragments after such *Eisenstein rotation* to produce masks for sharpening, smoothering and segmentation of images; the crucial point here is the invertibility of Eisenstein rotations. All the proposed algorithms have complexity $O(p^2)$ and can also be used for square-sampled digital images processing over *finite Gaussian fields* [8,9] or *complex discrete tori* [10–13], see also [14,15].

2. Finite Fields of Eisenstein Integers

Let $\mathbb{Z}$ and $\mathbb{C}$ be the ring of integers and the complex field respectively, let $\mathbb{Z}_n = \mathbb{Z}/n\mathbb{Z}$ be a residue class ring modulo an integer $n \geq 2$, and let $\mathbb{GF}(p^m)$ be a Galois field with p^m elements, where p is a prime and $m > 0$ is an integer.

In number theory [16, Ch. 1.4] a *Gaussian integer* is a complex number $z = a + bi \in \mathbb{C}$ whose real and imaginary parts are both integers. Further, *Eisenstein integers* are complex numbers of the form $z = a + b\omega$, where $a, b \in \mathbb{Z}$ and $\omega = \exp(2\pi i/3) \in \mathbb{C}$ is a primitive (non-real) cube root of unity, so that $\omega^3 = 1$ and $\omega^2 + \omega + 1 = 0$. Note that within the complex plane the Eisenstein integers may be seen to constitute a triangular lattice, in contrast with the Gaussian integers, which form a square lattice.

Both Gaussian and Eisenstein integers, with ordinary addition and multiplication of complex numbers, form, respectively, subrings $\mathbb{Z}[i]$ and $\mathbb{Z}[\omega]$ in the field $\mathbb{C}$. Unfortunately, lack of division in these rings significantly restricts its applicability to image processing problems [17]. So it is natural to look for finite fields, whose properties would be in some respect similar to properties of $\mathbb{Z}[i]$ and $\mathbb{Z}[\omega]$. In fact, it is known that if p is a prime number such that $p \equiv 3 \mod 4$, then the factor ring $\mathbb{C}(p) \stackrel{\text{def}}{=} \mathbb{Z}_p[x]/(x^2 + 1) \simeq \mathbb{GF}(p^2)$ is a "finite complex field". Its applications in analysis and in processing of square-sampled digital images have been considered in [8–12].

We may use the similar approach to construct "finite fields of Eisenstein integers" [18]. Indeed, it easy to show that if $p = 12k + 5$ is a prime, then the polynomial $x^2 + x + 1$ is irreducible over $\mathbb{Z}_p$ but $x^2 + 1 = 0$ is not.

Definition 1. Let $p \geq 5$ be a prime number such that $p \equiv 5 \pmod{12}$. Then the finite field

$$\mathbb{E}(p) \stackrel{\text{def}}{=} \mathbb{Z}_p[x]/(x^2 + x + 1) \simeq \mathbb{GF}(p^2)$$

will be called *Eisenstein field*. Elements of $\mathbb{E}(p)$ will be called *discrete Eisenstein numbers*.

Thus, Eisenstein fields have p^2 elements, where

$$p = 5, 17, 29, 41, 53, 89, 101, 113, 137, 149, 173, 197, 233, 257, \dots .$$

In particular, there are 44 fields $\mathbb{E}(p)$ for $5 \leq p < 1000$, and Fig. 2 demonstrates the smallest field $\mathbb{E}(5)$. Note that topologically $\mathbb{E}(p)$ is the *torus* $\mathbb{Z}_p \times \mathbb{Z}_p$, so that opposite sides of the diamond frame in Fig. 2 must be considered connected. The area inside the bold line (as is shown in Fig. 2) will be called the *main hexagon* of an Eisenstein field. Elements of $\mathbb{E}(p)$ are of the form $z = a + b\omega$, where $a, b \in \mathbb{Z}_p$ and ω denotes the class of residues of x, so that

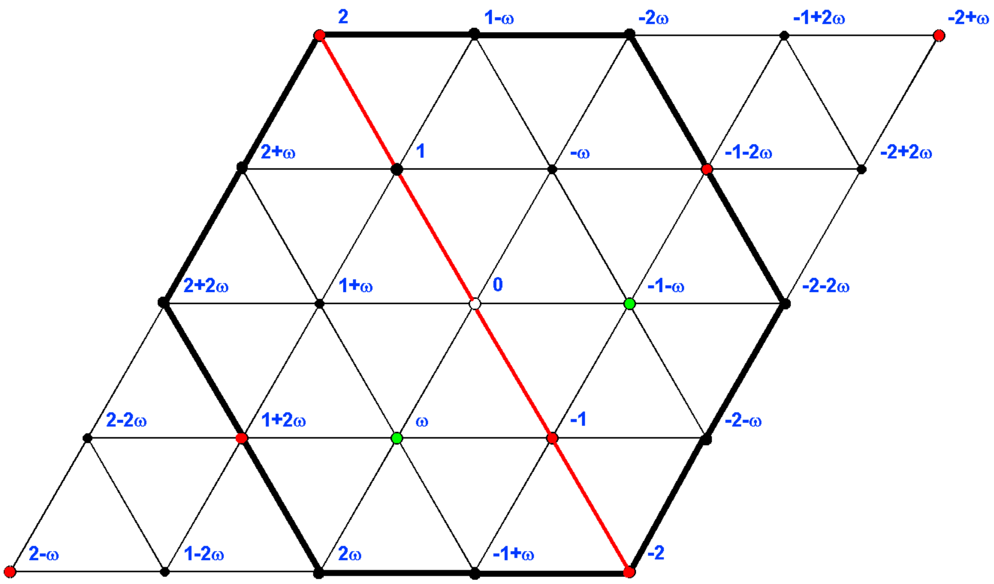

Fig. 2. The Eisenstein field $\mathbb{E}(5)$.

$\omega^2 + \omega + 1 = 0$. The product of $a + b\omega \in \mathbb{E}(p)$ and $c + d\omega \in \mathbb{E}(p)$ is given by

$$(a + b\omega)(c + d\omega) = (ac - bd) + (bc + ad - bd)\omega,$$

the addition is straightforward. The number $z^* = a + b\omega^2 = (a - b) - b\omega \in \mathbb{E}(p)$ is *conjugate* to z, and the product $zz^* = a^2 - ab + b^2 \in \mathbb{Z}_p$ is the *norm* $N(z)$ of z. (Note that in $\mathbb{E}(p)$ the concept of modulus $|z| = \sqrt{N(z)}$ is not defined.) It is easy to show that $N(z_1 z_2) = N(z_1)N(z_2)$ and $N(z) = 0 \Leftrightarrow z = 0$. Thus, nonzero elements $z \neq 0$ have inverses $z^{-1} = z^* N(z)^{-1}$, and so division is defined in $\mathbb{E}(p)$.

From now on we assume that the prime p satisfies the condition of Definition 1; moreover, where it cannot lead to misunderstanding, let us agree to identify residue classes of the field $\mathbb{Z}_p$ with their natural representatives.

3. Eisenstein Rotations of Hexagonal Images

Let $\mathbb{E}(p)$ be an Eisenstein field and let $f(z) : \mathbb{E}(p) \to \mathbb{R}$ be any real-valued function on $\mathbb{E}(p)$. Due to our geometric interpretation of Eisenstein fields, we call $f(z)$ a *hexagonal gray-level image of size* $p \times p$, or just *hexagonal image* briefly. It is natural to consider such images on the discrete torus $\mathbb{Z}_p \times \mathbb{Z}_p$. The upper left part of Fig. 3 gives an example of such image; the standard resampling algorithm [1, Sect. 6.1.1] has been used to embed the Lenna image into the Eisenstein field $\mathbb{E}(509)$. (Note that only for the sake of beauty we assume pixels outside the main hexagon of $\mathbb{E}(509)$ to be white.)

The algebraic operations in the field $\mathbb{E}(p)$ produce transforms of hexagonal images. For example, additions correspond to circular shifts. To be more precise, define for every $0 \neq w = a+b\omega \in \mathbb{E}(p)$ the transform $T_w : f(z) \to f(z+w)$. The image $T_w[f]$ is just the original image $f(z)$ shifted by a units along the "real" axis and by b units along the "complex" axis $O\omega$. The transform $T_w[f]$ of an image f will be called its *translation* by w.

Other transform $f(z) \to f(wz)$ produced by multiplication in $\mathbb{E}(p)$ is more interesting. Indeed, in the *continuous* complex plane, for any fixed $0 \neq w = re^{i\alpha} \in \mathbb{C}$ it is just composition of the rotation by an angle α about the origin O, with the r-scaling. Unfortunately, in discrete cases rotations and scalings are much more hard to define (see, for example, [19, p. 377] for square images and [1, p. 97], [6,7] for hexagonal images). Nevertheless, based on the analogy between $\mathbb{C}$ and $\mathbb{E}(p)$, one may expect that some properties of the transform $f(z) \to f(wz)$ could be similar to rotations even in the discrete case.

Definition 2. Let $w \in \mathbb{E}(p)$ be a nonzero discrete Eisenstein number. The transformation $R_w : f(z) \to f(wz)$ of a hexagonal image $f(z)$ will be called its *Eisenstein rotation* by w. In the special case $w = a+0\omega \in \mathbb{Z}_p$ it is an *Eisenstein scaling* by a.

We will look now at the transform in more details. Fig. 3 demonstrates some examples of Eisenstein rotations of the Lenna image over $\mathbb{E}(509)$ by

$$w = 1+\omega = -\omega^2, \quad w = (1+2\omega)^{-1} = -170+160\omega, \quad w = 1+2\omega, \quad w = (1+5\omega)^{-1} = 121+24\omega \quad \text{and} \quad w = 1+5\omega$$

respectively. Note that since the images are on the torus $\mathbb{Z}_{509}\times\mathbb{Z}_{509}$, the opposite sides of diamonds must be considered glued.

These and other examples demonstrate the following properties of Eisenstein rotations.

1. Since $\mathbb{E}(p)$ is a field, Eisenstein rotations are *invertible*: $R_w^{-1} = R_{w^{-1}}$. As a result, transformed image $R_w[f]$ keeps all the information about the original; in fact, the transform R_w is just a *permutation* of the original's pixels.
2. In general, Eisenstein rotations *do not preserve distances, angles and areas*, so that considerable distortions of images may occur.
3. Nevertheless, when p is large and when w is of the form $w = u^{-1}$ with a "small" $N(u)$, Eisenstein rotations do behave *similarly to continuous rotations*. Namely, then

   (a) the resulting image $R_w[f]$ consists of $N(u)$ fragments forming a tiling in the torus $\mathbb{Z}_p \times \mathbb{Z}_p$;
   (b) these fragments visually look like the original image $f(z)$ rotated by some angle and zoomed out at the rate $1/\sqrt{N(u)}$;
   (c) the "center" of one of the fragments coincides with the center of image f at the origin $0 \in \mathbb{E}(p)$.

Note that not all of these properties may be considered as rigorous mathematical statements and so some terms above have been put in quotes. Indeed, the first property immediately implies that all the fragments are composed by distinct pixels of the original image and so are *entirely different* as discrete objects. It means that only visual similarity of the fragments occur and so in general we may talk only about some *measure of similarity* between them. The six borders of hexagons with the Lenna image inside are in fact the following *disconnected* sets of dots in $\mathbb{E}(p)$:

$$X1 = \left\{kw + m(\omega^2 w - \omega^2) \ : \ k \in \mathbb{Z}_p\right\}, \qquad X2 = \left\{kw + m(\omega w - \omega^2) \ : \ k \in \mathbb{Z}_p\right\}, \qquad \text{(along the real axis)},$$

$$Y1 = \left\{k\omega w + m(\omega^2 w - \omega^2) \ : \ k \in \mathbb{Z}_p\right\}, \qquad Y2 = \left\{k\omega w + m(w - \omega^2) \ : \ k \in \mathbb{Z}_p\right\}, \qquad \text{(along the } O\omega \text{ axis)},$$

$$Z1 = \left\{k\omega^2 w - m(\omega w - \omega^2) \ : \ k \in \mathbb{Z}_p\right\}, \qquad Z2 = \left\{k\omega^2 w - m(w - \omega^2) \ : \ k \in \mathbb{Z}_p\right\}, \qquad \text{(along the } O\omega^2 \text{ axis)},$$

where $m = (p-1)/2$. The discontinuity can be seen in the right-hand side of Fig. 4.

Also, note that finite fields cannot be ordered and so such notions as “large” or “small” are meaningless in Eisenstein fields. Nevertheless, under the assumption of large p we may consider a *continuous model* of $\mathbb{E}(p)$, when *locally* we are treating representatives of residue classes as reals and using the ordinary arithmetic instead of modular operations. Based on such model, the appearance of small copies of the original image may be explained as follows. Note that discrete Eisenshtein numbers allow matrix representations

$$\mathbb{E}(p) \ni z = a + b\omega \leftrightarrow \mu(z) = \begin{pmatrix} a & -b \\ b & a-b \end{pmatrix} \in \mathbb{M}_2(\mathbb{Z}_p), \qquad \det \mu(z) = a^2 - ab + b^2 = N(z),$$

where determinants of matrices are just norms of corresponding Eisenshtein numbers. Thus, $N(w)$ may be considered as the Jacobian of Eisenshtein rotation R_w. Examples in Fig. 3 demonstrate that the standard interpretation of the Jacobian in continuous cases as the *area distortion factor* to some extent may be transferred to finite Eisenshtein fields. Indeed, according to the continuous model, the area of the image f under the Eisenshtein rotation R_w with $N(w) = 1/N(u)$ must shrinks $N(u)$ times. But R_w just permutes pixels, so that $N(u)$ fragments must appear. At the same time, imperfections of the continuous model clearly follows from the fact that in general the total number of pixels p^2 is not divisibe by $N(u)$, so that the fragments *cannot contain the same number of pixels*.

To explain similarity of fragments, consider a small neighbourhood $V(z_0)$ of any fixed point $z_0 \in \mathbb{E}(p)$. Then, in the frame of the continuous model, the norm $N(z - z_0) = n$ must also be small for $z \in V(z_0)$. On the other hand, $N(w(z - z_0)) = nN(w) = N(wz - wz_0)$ and so for $N(w) = s/n$ holds $N(w(z - z_0)) = s$. In other words,

> under the Eisenshtein rotation R_w, the image wz of a point $z \in V(z_0)$ will be in a vicinity of wz_0 if $N(w)N(z - z_0)$ is “small”.

Example. Let $u = 1 + 2\omega \in \mathbb{E}(257)$ and let $w = 1/u = -86 + 85\omega \in \mathbb{E}(257)$. Then $N(u) = 3$ and $N(w) = \frac{1}{3} = 86$ (mod 287). Consider the following neighbourhood of an arbitrary point $z_0 \in \mathbb{E}(257)$:

$$V(z_0) = \left\{a + ib - z_0 \ : \ -2 \le a, b \le 2\right\}.$$

Let $V = V(0)$. Evidently, 0 is the only fixed point under rotations, and the other 24 points in V have 1, 3, 4, 7 and 12 as their norms. Let U_0 be the set of 9 points with norms 3 or 12. For $z = 1 - \omega \in V$ with $N(z) = 3$ we have $wz = -1 - \omega \in V$; indeed, $N(wz) = 1$. Similarly, for $z = 2 - 2\omega \in V$ with $N(z) = 12$ we have $N(wz) = \frac{12}{3} = 4$ and so again $wz = -2 - 2\omega \in V$. Other points in V with images also in V, are $-1 + \omega$, $-2 + 2\omega$, $\pm(2 + \omega)$ and $\pm(1 + 2\omega)$.

Now let $z = 1 - 2\omega \in V$ with $N(z) = 7$. Then

$$wz = \frac{z}{u} = \frac{zu^*}{N(u)} = \frac{(1 - 2\omega)(1 + 2\omega^2)}{3} = -86(5 + 4\omega) = -430 - 344\omega = 84 - 87\omega \in \mathbb{E}(257)$$

and so $wz \notin V$ but $wz \in V(-w) = V(86 - 85\omega)$. In fact, let U_{-1} be the following set of 8 points:

$$U_{-1} = \left\{ -1,\ 2,\ -\omega,\ 2\omega,\ 1 + \omega,\ 1 - 2\omega,\ -2 + \omega,\ -2 - 2\omega \right\}.$$

Images of all the points from U_{-1} are in the neighbourhood $V(-w)$, i.e., $wU_{-1} \subset V(-w)$. Similarly, if $U_1 = -U_{-1}$ contains all the points from U_{-1} with opposite signs, then $wU_1 \subset V(w)$.

We may summarize as follows. Let f be a binary image of 5×5-square on $\mathbb{E}(257)$, with $f(z) = 1$ for $z \in V(0)$, and $f(z) = 0$ otherwise. Then the Eisenstein rotation $R_w[f]$ of f consists of three separate fragments wU_0, wU_1 and wU_{-1}, localized near the points 0, w and $-w$ respectively.

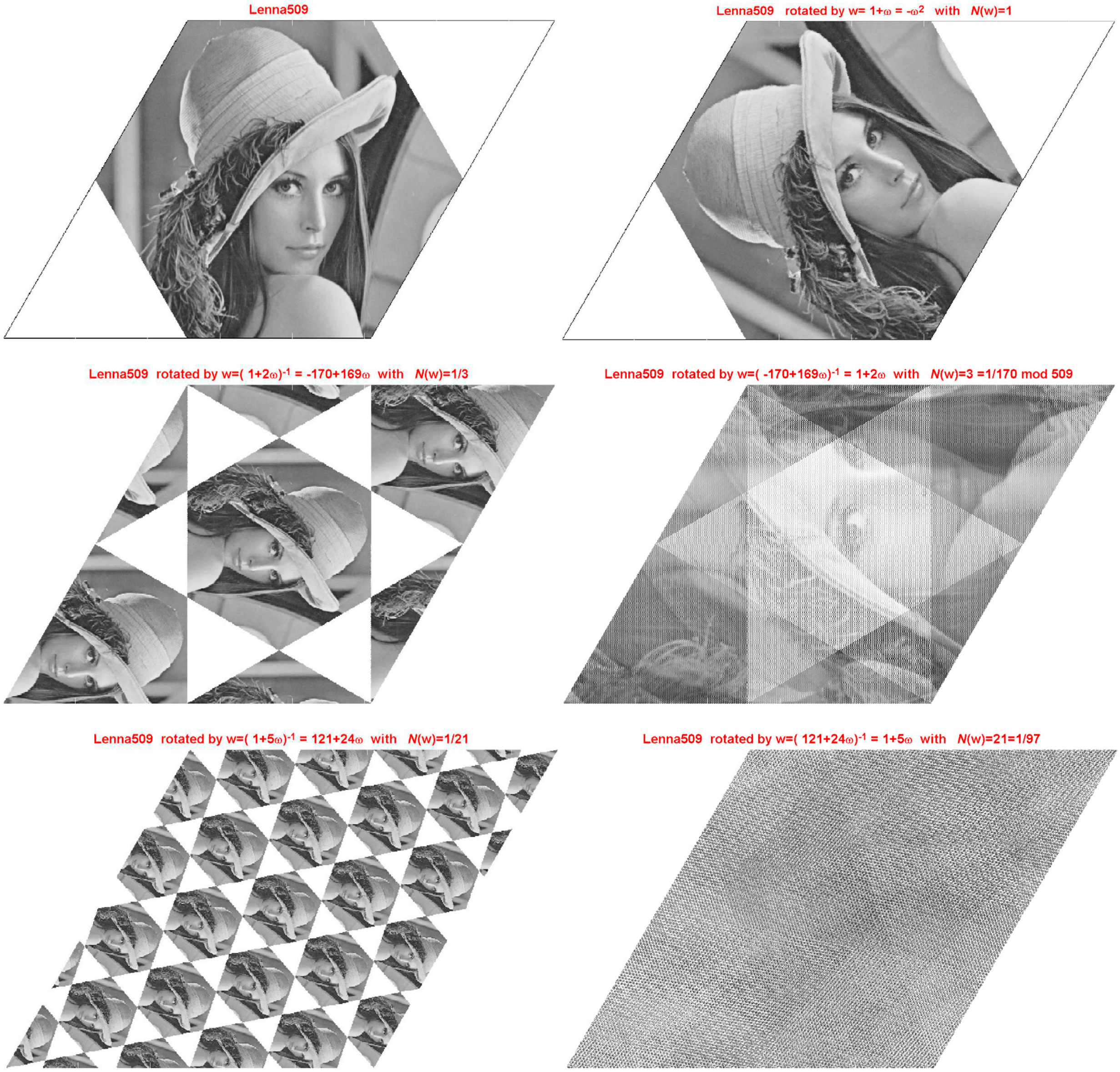

Fig. 3. Examples of Eisenstein rotations of the hexagonal image of Lenna over $\mathbb{E}(509)$.

4. Hexagonal Images Enhancement Based on Eisenstein Rotations

The fact that Eisenshtein rotations split images into visually similar fragments can be used for sharpening, smoothering and segmentation of the images. Indeed, as it has been discussed in Section 3, in the frame of the continuous model Eisenstein rotation $R_w[f]$ may be considered as a regular tiling spanned by any two from the vectors $\mathbf{v_1}$, $\mathbf{v_2}$ and $\mathbf{v_3}$, see Fig. 4. Then one can shift *any* fragment to the center and reverse the Eisenshtein rotation afterwards. The result will be similar but not identical to the original image and can be used to produce a mask for its enhancement, see [20, Sect. 10.4.1].

To be more precise, assume that a prime p is sufficiently large (say, $p \geq 257$), $w = u^{-1} \in \mathbb{E}(p)$ and $n = N(u) \in \mathbb{Z}$ is small (say, $n < 30$). Assume that vectors $\mathbf{v_1}$ and $\mathbf{v_2}$ span the tiling of the torus, and let $\mathbf{v} = r\mathbf{v_1} + s\mathbf{v_2}$, where $r, s \in \mathbb{Z}$. Then the translation $T_{\mathbf{v}}$ circularly shifts fragments of $R_w[f]$ (r times along the $\mathbf{v_1}$-direction and s times along $\mathbf{v_2}$).

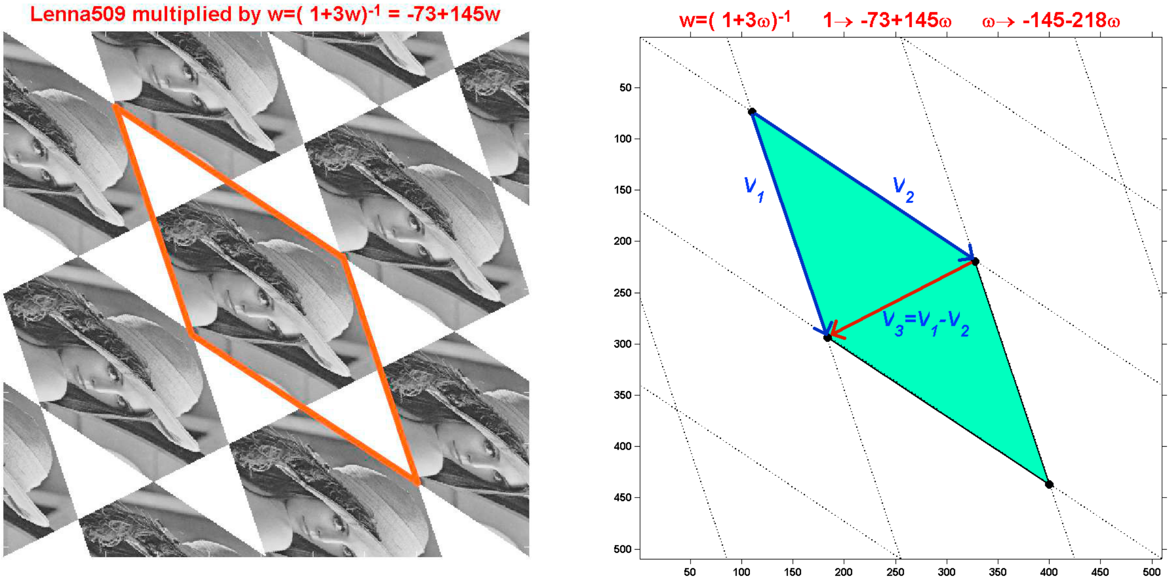

Fig. 4. The continuous model of the tiling produced by $R^{-1}_{1+3\omega} \in \mathbb{E}(509)$.

Definition 3. The image

$$M_{r,s,w}[f] = f - R_w^{-1} T_{\mathbf{v}} R_w[f], \qquad \text{where } \mathbf{v} = r\mathbf{v_1} + s\mathbf{v_2},$$

will be called *Eisenstein mask* or just *mask*.

Note that there are precisely n different masks for any fixed w, so that the coefficients r and s cannot be chosen independently of each other. Also, note that pixels of a mask could be both negative and positive. For example, let $p = 509$ and let f be the Lenna image over the Eisenstein field $\mathbb{E}(509)$, see Fig. 5(a). The mask $M_{1,-1,w}[f]$ for $w = (2+\omega)^{-1}$, $\mathbf{v_1} = w$ and $\mathbf{v_2} = w\omega$ is shown in Fig. 5(e). (The intensity range of the mask is $[-164, 218]$, so that the background is gray.) Its modulus $\left|M_{1,-1,w}[f]\right|$ in Fig. 5(f) demonstrates the "pencil drawing" effect.

The transforms

$$H_1[f] = f + \alpha M[f] = 2f - \alpha R_w^{-1} T_{\mathbf{v}} R_w[f] \qquad \text{and} \qquad H_2[f] = f + \alpha\left|M[f]\right|, \quad \text{where } M = M_{r,s,w} \text{ and } \alpha \in \mathbb{R},$$

may be used to produce different sharpening effects. Results will depend on the parameters w, $\mathbf{v}$ and α; in general, rotations by w with smaller $n = N(w^{-1})$ would produce finely output. For example, Fig. 5(c) is the sum of the original image (at the top) with the mask $M_{1,-1,2+\omega}[f]$ (just below). The image Fig. 5(b) has been produced by $w = 1 + 3\omega$, $\alpha = 1$, $r = 1$ and $s = 0$.

Different masks can be combined and the image in Fig. 5(d) has been produced as $f + M$, where

$$M = \left|M_{1,0,w}[f]\right| + \left|M_{0,1,w}[f]\right|, \qquad \text{with } w = 1 + 3\omega \text{ and } n = 7.$$

is the sum of absolute values of two masks. We may observe quite a coarse effect more suitable for segmentation purposes. Finally, the transform

$$R_w^{-1}\left(\sum_{r,s} \alpha_{rs} T_{r\mathbf{v_1}+s\mathbf{v_2}}\right) R_w$$

can be used for smoothering of images.

All the proposed methods can be realized with complexity $O(p^2)$ and may be used also for the processing over finite Gaussian fields of square-sampled digital images.

(a)

(b)

(c)

(d)

(e)

(f)

Fig. 5. Examples of sharpening and lining by Eisenstein rotations.

5. Conclusion

This paper proposes an algebraic method for the processing of hexagonally sampled images, based on their representation as functions on special finite fields, called "Eisenstein fields". Some properties of such fields are studied; in particular, it is shown that its elements are in natural correspondence with hexagons in a $(p \times p)$-diamond-shaped fragment of a regular plane tiling. The concept of Eisenstein rotation is introduced and some its properties are studied. Based on Eisenstein rotations, some methods for sharpening, smoothering and segmentation of hexagonal images are proposed. However, apart from of this work, there remain issues such as the detailed study of properties of the introduced transformations, the study of possibilities of its generalizations, as well as the details of its practical applications including estimation of image processing quality in the presence of noise. Authors hope to return to the study of these issues in the further papers.

Acknowledgements

This research has been partially supported by the Russian Foundation for Basic Research grant no. 16-07-00648-a. The authors would like to thank the anonymous reviewer for constructive comments and suggestions.

References

[1] L. Middleton, J. Sivaswamy, Hexagonal Image Processing: A Practical Approach, Springer-Verlag, London, 2005.
[2] S. Coleman, B. Scotney, B. Gardiner, Integral spiral image for fast hexagonal image processing, in: A. Petrosino (Ed.), Proceedings of the 17-th International Conference on Image Analysis and Processing (ICIAP-2013), Naples, Italy, September 9–13, 2013, volume 8157 of *Lecture Notes in Computer Science*, Springer-Verlag Berlin Heidelberg, 2013, pp. 532–541. doi:10.1007/978-3-642-41184-7_54.
[3] K. Mostafa, J. Chiang, I. Her, Edge-detection method using binary morphology on hexagonal images, The Imaging Science Journal 63 (2015) 168–173.
[4] B. Kumar, P. Gupta, K. Pahwa, Square pixels to hexagonal pixel structure representation technique, Int. Journal of Signal Processing, Image Processing and Pattern Recognition 7 (2014) 137–144.
[5] R. Mersereau, The processing of hexagonally sampled two-dimensional signals, Proc. IEEE. 67 (1979) 930–949.
[6] X. He, W. Jia, N. Hur, Q. Wu, J. Kim, Image translation and rotation on hexagonal structure, in: The 6th IEEE International Conference on Computer and Information Technology (CIT'06), Seoul, Korea, September 20-22, 2006, p. 141. doi:10.1109/CIT.2006.201.
[7] I. Her, Geometric transforms on the hexagonal grid, IEEE Transactions on Image Processing 4 (1995) 1213–1922.
[8] J. Bandeira, R. Campello de Souza, New trigonometric transforms over prime finite fields for image filtering, in: Proc. of the 6th International Telecommunications Symposium (ITS2006), Fortaleza-Ce, Brazil, September 3-6, 2006, pp. 628–633. doi:10.1109/ITS.2006.4433235.
[9] R. Campello de Souza, H. de Oliveira, D. Silva, The Z-transform over finite fields, 2015. URL: `https://arxiv.org/pdf/1502.03371`, arXiv preprint published online 11th February 2015.
[10] V. Mnukhin, Transformations of digital images on complex discrete tori, Pattern Recognition and Image Analysis 24 (2014) 552–560.
[11] V. Mnukhin, Digital images on a complex discrete torus, Journal of Machine Learning and Data Analysis 1 (2013) 542–551. (In Russian).
[12] V. Mnukhin, Fourier-Mellin transform on a complex discrete torus, in: Y. I. Zhuravlev, et al. (Eds.), Proc. of the 11th Int. Conf. "Pattern Recognition and Image Analysis: New Information Technologies" (PRIA-11-2013), Samara, Russia, September 23–28, 2013, volume 11 of *Pattern Recognition and Image Analysis*, IPSI RAS Samara, 2013, pp. 102–105. doi:10.13140/RG.2.1.4366.4086.
[13] A. Karkishchenko, V. Mnukhin, Applications of modular logarithms on complex discrete tori in digital image processing, Bulletin of the Rostov State Transport University 3 (2013) 147–153. (In Russian).
[14] V. Labunets, Number theoretic transforms over quadratic fields, Complex Control Systems, Institute of Cybernetics USSR, Kiev, 1982, pp. 30–37. (In Russian).
[15] L. Varitschenko, V. Labunets, M. Rakov, Abstract Algebraic Systems and Digital Signal Processing, Naukova Dumka, Kiev, 1986. (In Russian).
[16] K. Ireland, M. Rosen, A Classical Introduction to Modern Number Theory, volume 84 of *Graduate Texts in Mathematics*, Springer, New York, 1990.
[17] H. G. Baker, Complex Gaussian integers for "Gaussian graphics", SIGPLAN Not. 28 (1993) 22–27.
[18] A. Karkishchenko, V. Mnukhin, Threefold symmetry detection in hexagonal images based on finite Eisenstein fields, in: D. Ignatov, et al. (Eds.), Analysis of Images, Social Networks and Texts: 5th International Conference (AIST 2016), Yekaterinburg, Russia, April 7-9, 2016, volume 661 of *Communications in Computer and Information Science*, Springer, Cham, 2017, pp. 281–292. doi:10.1007/978-3-319-52920-2_26.
[19] A. Karkishchenko, V. Mnukhin, Topological filtration for digital images recognition and symmetry analysis, Journal of Machine Learning and Data Analysis 1 (2014) 966–987. (In Russian).
[20] W. K. Pratt, Introduction to Digital Image Processing, CRC Press, Boca Raton, FL, 2014.
[21] A. Rubis, M. Lebedev, Y. Vizilter, O. Vygolov, Morphological image filtering based on guided contrasting, Computer Optics 40 (2016) 73–79.
[22] M. Gashnikov, N. Glumov, A. Kuznetsov, V. Mitekin, V. Myasnikov, V. Sergeev, Hyperspectral remote sensing data compression and protection, Computer Optics 40 (2016) 689–712.